

Femtocells in Centralized Systems: Green Operation and Radio Resource Management Techniques

Elias Yaacoub

Received: date / Accepted: date

Abstract In this paper, a system of femtocells controlled by a single controller is investigated. In such a scenario, femtocell access points (FAPs) are assumed connected via wired links to a central controller within a certain vicinity (e.g. building, compound, hotel, campus, etc.). Thus, radio resource management (RRM) and green network operation of LTE femtocell networks are investigated in an integrated wired/wireless system. Consequently, it becomes possible to perform RRM in a centralized and controlled way in order to enhance the quality of service (QoS) performance for the users in the network. Furthermore, energy efficient operation consisting of switching off redundant FAPs can be implemented. A utility maximization framework is presented, and an RRM algorithm that can be used to maximize various utility functions is proposed. Another algorithm is presented for the scenario of FAP on/off switching to achieve green operation. It consists of selecting the best FAP to switch off, then moving the femto user equipments (FUEs) to other active FAPs without compromising their quality of service (QoS). Simulation results show that the proposed algorithms lead to significant performance gains.

Keywords Femtocell · energy efficiency · resource allocation · interference mitigation · LTE

1 Introduction

The proliferation of small cells, notably femtocells, is expected to increase in the coming years [2]. Since most of the wireless traffic is initiated indoors, Femtocell

Part of this work was published in [1].

Elias Yaacoub
Faculty of Computer Studies
Arab Open University - Lebanon
Tel.: +961-4-404101 Ext.:439
E-mail: eliasy@ieee.org

Access Points (FAPs) are designed to handle this traffic and reduce the load on macrocell base stations (BSs). They are small, low power, plug and play devices providing indoor wireless coverage to meet the quality of service (QoS) requirements for indoor data users [3]. FAPs are generally installed inside home or office of a given subscriber, and are connected to the mobile operator's core network via wired links, e.g. digital subscriber line (DSL) [4]. However, they are not under the direct control of the mobile operator since they are not connected to neighboring macrocell BSs (MBSs) through the standardized interfaces, e.g., the X2 interface for the long term evolution (LTE) cellular system.

Therefore, a main challenge is to control the overall interference level in the network that depends on the density of small cells and their operation, and may affect the configuration of macrocell sites [5]. In [6], this problem was addressed by proposing macrocell-femtocell cooperation, where a femtocell user may act as a relay for macrocell users, and in return each cooperative macrocell user grants the femtocell user a fraction of its superframe. In [7], it was assumed that both macrocells and small cells are controlled by the same operator, and it was shown that in this case the operator can control the system load by tuning pricing and bandwidth allocation policy between macrocells and small cells.

On the other hand, other works investigated radio resource management (RRM) in femtocell networks by avoiding interference to/from macrocells. Most of these works focused on using cognitive radio (CR) channel sensing techniques to determine channel availability. In [8], femtocells use cognitive radio to sense the spectrum and detect macrocell transmissions to avoid interference. They perform radio resource management on the free channels. However, there is a time dedicated for sensing the channel that cannot overlap with transmission/RRM time. A channel sensing approach for improving the capacity of femtocell users in macro-femto overlay networks is proposed in [9]. It is based on spatial radio resource reuse based on the channel sensing outcomes. In [10], enhanced spectrum sensing algorithms are proposed for femtocell networks in order to ensure a better detection accuracy of channels occupied by macrocell traffic.

The main competitor for indoor femtocells is naturally the widely deployed WiFi IEEE 802.11 family of standards. Although WiFi is cheaper and currently ubiquitous, it uses free spectrum in the industrial, scientific, and medical (ISM) band, which makes it vulnerable to uncontrolled transmissions in the same band. On the other hand, femtocells appear to FUEs as cellular BSs, and the signaling, access control, and radio resource management techniques follow those of the cellular network. They also generally use the licensed cellular spectrum, which avoids unwanted interference from devices accessing open spectrum like the ISM band. Thus, femtocells act as a natural extension of the cellular network and allow seamless roaming [11].

Recent standardization for LTE Release 13 and 14 have considered carrier aggregation (CA) between a licensed LTE carrier and small cells using unlicensed spectrum. This approach is called licensed assisted access (LAA) in the LTE standard. LAA cells will have to coexist with WiFi cells by using a mechanism for channel sensing. Furthermore, the coexistence of LAA LTE cells with WiFi access points was shown to provide a boost to WiFi performance, compared to the coexistence of two WiFi networks [12].

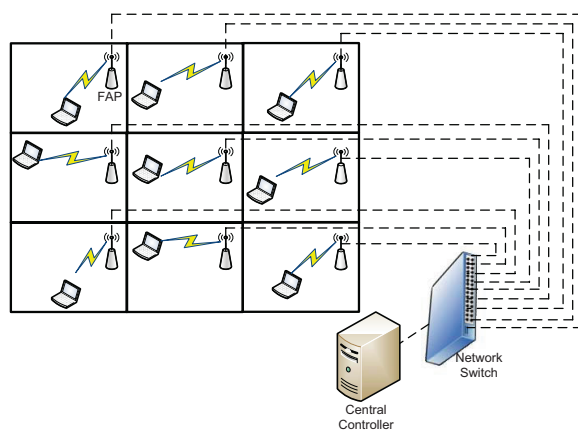


Fig. 1 System model.

In this paper, LTE femtocell networks are investigated. FAPs are not assumed to be controlled by the mobile operator. However, in certain scenarios, FAPs at a given location can be controlled by a single entity. This can happen, for example, in a university campus, hotel, housing complex, or office building. In such scenarios, in addition to the wireless connection between FAPs and mobile terminals (MTs), FAPs can be connected via a wired high-speed network to a central controller within the building or campus. This can allow more efficient RRM decisions leading to significant QoS enhancements for mobile users. Furthermore, it can allow energy efficient operation of the network, by switching off unnecessary FAPs whenever possible, and serving their active FUEs from other neighboring FAPs that still can satisfy their QoS requirements. Due to centralized control, users do not have to worry about opening the access to their FAPs for FUEs within the premises, since the controller will guarantee the QoS. This scenario is studied in this paper, where two algorithms are presented: A utility maximizing RRM algorithm to perform resource allocation over the FAPs controlled by the same entity, and an algorithm for the green operation of LTE femtocell networks via on/off switching. Significant gains are shown to be achieved under this integrated wired/wireless scenario compared to the case where each FAP acts independently.

The paper is organized as follows. The system model is presented in Section 2. The utility metrics leading to different QoS and performance targets are described in Section 3. The joint RRM algorithm implemented at the central controller is presented in Section 4, and the FAP on/off switching algorithm is presented in Section 5. Simulation results are presented and analyzed in Section 6. Finally, conclusions are drawn in Section 7.

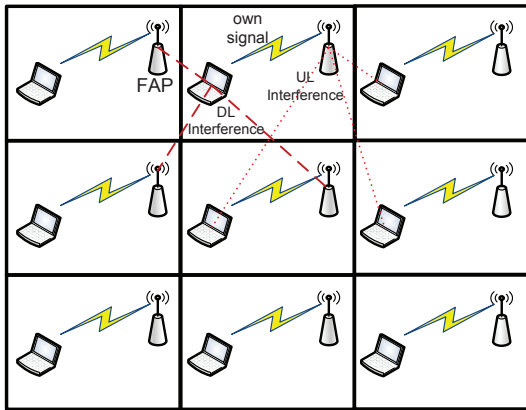


Fig. 2 Intercell interference in the uplink and downlink.

2 System Model

The system model is shown in Fig. 1. As an example, a building having three apartments per floor is considered. One FAP is available in each apartment, primarily to serve the FUEs available in that apartment. The FAPs are connected to FUEs over the air interface, but they are connected via a wired network (dashed lines in Fig. 1) to a central controller located within the building (for example, in a room hosting telecom/networking equipment in the basement).

Interference is caused by the transmissions of a FAP to the users served by the other FAPs in other apartments. In the downlink (DL) direction from the FAPs to the FUEs, interference is caused by the transmissions of a FAP to the FUEs served by the other FAPs in other apartments, as shown by the dashed lines in Fig. 2, representing the interference on the FUE in the second apartment in the third floor from the FAPs in neighboring apartments. In the uplink (UL) direction from the FUEs to the FAPs, interference is caused by the transmissions of an FUE to the FAPs in other apartments, as shown by the dotted lines in Fig. 2, representing the interference on the second FAP in the third floor from the FUEs in neighboring apartments. Centralized RRM in an integrated wired/wireless scenario, as shown in Fig. 1, can be used to mitigate the impact of interference and enhance QoS performance. In addition, centralized control allows to switch certain FAPs off, or put them in sleep mode, when they are not serving any FUEs, or when the FUEs they serve can be handed over to other neighboring FAPs within the same building, without affecting their QoS. The main contribution of this paper, detailed in section 5, is proposing an algorithm to implement this green switching approach.

In the absence of the central controller and wired connections between FAPs, each FAP would act independently, without being aware of the network conditions

within the coverage areas of other FAPs. Thus, each FAP would selfishly serve its own FUEs, regardless of the interference caused to other FUEs, or the redundant energy consumption.

The building of Fig. 1 is assumed to be within the coverage area of an MBS, positioned at a distance d_{BS} from the building. The interference from the MBS to the FAPs is taken into account in the analysis: it is assumed in this paper that the MBS is fully loaded, i.e. all its resource blocks (RBs) are occupied, which causes macro interference to all the FAPs in the building. No coordination is assumed between the mobile operator of the MBS and the central controller of the building FAPs.

Energy efficient FAP switching in conjunction with intelligent RRM is considered in this paper within the framework of LTE. The downlink direction (DL) from the FAPs to the FUEs is studied, although the presented approach can be easily adapted to the uplink (UL) direction from the FUEs to the FAPs. In LTE, orthogonal frequency division multiple access (OFDMA) is the access scheme used for DL communications. The spectrum is divided into RBs, with each RB consisting of 12 adjacent subcarriers. The assignment of an RB takes place every 1 ms, which is the duration of one transmission time interval (TTI), or, equivalently, the duration of two 0.5 ms slots [13, 14]. LTE allows bandwidth scalability, where a bandwidth of 1.4, 3, 5, 10, 15, and 20 MHz corresponds to 6, 15, 25, 50, 75, and 100 RBs, respectively [14]. In this paper, scenarios where the MBS and the FAPs are using the same bandwidth are assumed (i.e. a frequency reuse of one where bandwidth chunks in different cells are not orthogonal).

2.1 Channel Model

The pathloss between user k_l (connected to FAP l) and FAP j is given by [15]:

$$PL_{k_l,j,\text{dB}} = 38.46 + 20 \log_{10} d_{k_l,j} + 0.3d_{k_l,j} + 18.3n^{((n+2)/(n+1)-0.46)} + qL_{iw} \quad (1)$$

where $d_{k_l,j}$ is the indoor distance between user k_l and FAP j , n is the number of floors separating user k_l and FAP j , q is the number of walls between apartments, and L_{iw} is a per wall penetration loss. In (1), the first term $38.46 + 20 \log_{10} d_{k_l,j}$ is the distance dependent free space path loss, the term $0.3d_{k_l,j}$ models indoor distance dependent attenuation, the term $18.3n^{((n+2)/(n+1)-0.46)}$ indicates losses due to propagation across floors, and qL_{iw} corresponds to losses across apartment walls in the same floor. In this paper, $L_{iw} = 5$ dB is used as recommended in [15]. The pathloss between user k_l and its serving FAP l is a special case of (1), with $j = l$, $n = 0$, and $q = 0$.

The FAPs in this paper are assumed to be numbered from $j = 1$ to $j = L$, and the outdoor MBS is represented by $j = 0$. The pathloss between user k_l connected to FAP l and the MBS $j = 0$ is given by [15]:

$$PL_{k_l,j,\text{dB}} = 15.3 + 37.6 \log_{10} d_{\text{out},k_l,j} + 0.3d_{\text{in},k_l,j} + qL_{iw} + L_{ow} \quad (2)$$

where $d_{\text{out},k_l,j}$ is the distance traveled outdoor between the MBS and the building external wall, $d_{\text{in},k_l,j}$ is the indoor traveled distance between the building wall and

user k_l , and L_{ow} is an outdoor-indoor penetration loss (loss incurred by the outdoor signal to penetrate the building). It is set to $L_{ow} = 20$ dB [15]. In this paper, the MBS is considered to be located at a distance d_{BS} from the building. Thus, the indoor distance can be considered negligible compared to the outdoor distance. Furthermore, the MBS is assumed to be facing the building of Fig. 2, such that $q = 0$ can be used. Thus, the outdoor-indoor propagation model of (2) becomes:

$$PL_{k_l,j,\text{dB}} = 15.3 + 37.6 \log_{10} d_{k_l,j} + L_{ow} \quad (3)$$

Taking into account fading fluctuations in addition to pathloss, the channel gain between user k_l and FAP/MBS j can be expressed as:

$$H_{k_l,i,j,\text{dB}} = -PL_{k_l,j,\text{dB}} + \xi_{k_l,j} + 10 \log_{10} F_{k_l,i,j} \quad (4)$$

where the first factor captures propagation loss, according to (1) or (2)-(3). The second factor, $\xi_{k_l,j}$, captures log-normal shadowing with zero-mean and a standard deviation σ_ξ (set to $\sigma_\xi = 8$ dB in this paper), whereas the last factor, $F_{k_l,i,j}$, corresponds to Rayleigh fading power between user k_l and FAP or BS j over RB i , with a Rayleigh parameter b such that $E\{|b|^2\} = 1$. It should be noted that fast Rayleigh fading is assumed to be approximately constant over the subcarriers of a given RB, and independent identically distributed (iid) over RBs.

The pathloss model of [15], initially proposed for device-to-device (D2D) communications in LTE-Advanced (LTE-A), is selected for the femtocell scenario in this paper, due to important similarities between the two scenarios. In fact, the model corresponds to relatively short distance between transmitter and receiver, and considers comparable heights between them, as opposed to pathloss models suitable for macrocell scenarios, where the BS is at a significantly higher position than the UE. Furthermore, in addition to indoor propagation, the model takes into account outdoor propagation and outdoor-indoor penetration loss, which makes it very suitable to model interference to/from macrocell BSs.

2.2 Calculation of the Data Rates

Letting $\mathcal{I}_{\text{sub},k_l}$ and $\mathcal{I}_{\text{RB},k_l}$ be the sets of subcarriers and RBs, respectively, allocated to user k_l in femtocell l , N_{RB} the total number of RBs, L the number of FAPs, K_l the number of users connected to FAP l , $P_{i,l}$ the power transmitted over subcarrier i by FAP l , $P_{l,\text{max}}$ the maximum transmission power of FAP l , and R_{k_l} the achievable data rate of user k_l in femtocell l , then the OFDMA throughput of user k_l in femtocell l is given by:

$$R_{k_l}(\mathbf{P}_l, \mathcal{I}_{\text{sub},k_l}) = \sum_{i \in \mathcal{I}_{\text{sub},k_l}} B_{\text{sub}} \cdot \log_2(1 + \beta \gamma_{k_l,i,l}) \quad (5)$$

where B_{sub} is the subcarrier bandwidth expressed as $B_{\text{sub}} = \frac{B}{N_{\text{sub}}}$, with B the total usable bandwidth, and N_{sub} the total number of subcarriers. In (5), β refers to the signal to noise ratio (SNR) gap. It indicates the difference between the SNR needed to achieve a certain data transmission rate for a practical M-QAM (quadrature amplitude

modulation) system and the theoretical limit (Shannon capacity) [16]. It is given by $\beta = \frac{-1.5}{\ln(5P_b)}$, where P_b denotes the target bit error rate (BER), set to $P_b = 10^{-6}$ in this paper.

In addition, in (5), \mathbf{P}_1 represents a vector of the transmitted power on each subcarrier by FAP/MBS l , $P_{i,l}$. In this paper, the transmit power is considered to be equally allocated over the subcarriers. Hence, for all i , we have $P_{i,l} = \frac{P_{l,\max}}{N_{\text{sub}}}$.

The signal to interference plus noise ratio (SINR) of user k_l over subcarrier i in cell l in the DL, $\gamma_{k_l,i,l}$, is expressed as:

$$\gamma_{k_l,i,l} = \frac{P_{i,l}H_{k_l,i,l}}{I_{i,k_l} + \sigma_{i,k_l}^2} \quad (6)$$

where σ_{i,k_l}^2 is the noise power over subcarrier i in the receiver of user k_l , and I_{i,k_l} is the interference on subcarrier i measured at the receiver of user k_l . The expression of the interference is given by:

$$I_{i,k_l} = \sum_{j \neq l, j=0}^L \left(\sum_{k_j=1}^{K_j} \alpha_{k_j,i,j} \right) \cdot P_{i,j}H_{k_l,i,j} \quad (7)$$

In (7), K_j is the number of FUEs served by FAP j , and $\alpha_{k_j,i,j}$ is a binary variable representing the exclusivity of subcarrier allocation: $\alpha_{k_j,i,j} = 1$ if subcarrier i is allocated to user k_j in cell j , i.e., $i \in \mathcal{I}_{\text{sub},k_j}$, and $\alpha_{k_j,i,j} = 0$ otherwise. In fact, in each cell, an LTE RB, along with the subcarriers constituting that RB, can be allocated to a single user at a given TTI. Consequently, the following is verified in each cell j :

$$\sum_{k_j=1}^{K_j} \alpha_{k_j,i,j} \leq 1 \quad (8)$$

The term corresponding to $j = 0$ in (7) represents the interference from the MBS, whereas the terms corresponding to $j = 1$ to $j = L$ represent the interference from the other FAPs in the building.

3 Network Utility Maximization

In this section, the problem formulation for maximizing the network utility is presented. In addition, different utility metrics leading to different QoS objectives are presented and discussed.

3.1 Problem Formulation

With $U^{(l)}$ and U_{k_l} denoting the utility of FAP l and user k_l , respectively, such that $U^{(l)} = \sum_{k_l=1}^{K_l} U_{k_l}$, then the objective is to maximize the total utility in the network of Fig. 1, $\sum_{l=1}^L U^{(l)}$:

$$\max_{\alpha_{k_l,i,l}, P_{i,l}} U_{\text{tot}} = \sum_{l=1}^L U^{(l)} \quad (9)$$

Subject to:

$$\sum_{i=1}^{N_{\text{sub}}} P_{i,l} \leq P_{l,\text{max}}; \forall l = 1, \dots, L \quad (10)$$

$$\sum_{k_l=1}^{K_l} \alpha_{k_l,i,l} \leq 1; \forall i = 1, \dots, N_{\text{sub}}; \forall l = 1, \dots, L \quad (11)$$

The constraint in (10) indicates that the transmit power cannot exceed the maximum FAP transmit power, whereas the constraint in (11) corresponds to the exclusivity of subcarrier allocation in each femtocell, since in each LTE cell, a subcarrier can be allocated at most to a unique user at a given scheduling instant. Different utility functions depending on the users' data rates are described next.

3.2 Utility Selection

The utility metrics investigated include Max C/I, proportional fair (PF), and Max-Min utilities. The impact of their implementation on the sum-rate, geometric mean, maximum and minimum data rates in the network is studied in Section 6.1 using the Algorithm of Section 4.

3.2.1 Max C/I Utility

Letting the utility equal to the data rate $U_k = R_k$, the formulation in (9) becomes a greedy maximization of the sum-rate in the network. This approach is known in the literature as Max C/I. However, in this case, users with favorable channel and interference conditions will be allocated most of the resources and will achieve very high data rates, whereas users suffering from higher propagation losses and/or interference levels will be deprived from RBs and will have very low data rates.

3.2.2 Max-Min Utility

Due to the unfairness of Max C/I resource allocation, the need for more fair utility metrics arises. Max-Min utilities are a family of utility functions attempting to maximize the minimum data rate in the network, e.g., [17, 18]. A vector \mathbf{R} of user data rates is Max-Min fair if and only if, for each k , an increase in R_k leads to a decrease in R_j for some j with $R_j < R_k$ [17]. By increasing the priority of users having lower rates, Max-Min utilities lead to more fairness in the network. It was shown that Max-Min fairness can be achieved by utilities of the form [18]:

$$U_k(R_k) = -\frac{R_k^{-a}}{a}, a > 0 \quad (12)$$

where the parameter a determines the degree of fairness. Max-Min fairness is attained when $a \rightarrow \infty$ [18]. we use $a = 10$ in this paper. However, enhancing the worst case performance could come at the expense of users with good channel conditions (and who could achieve high data rates) that will be unfavored by the RRM algorithms

in order to increase the rates of worst case users. A tradeoff between Max C/I and Max-Min RRM can be achieved through proportional fair (PF) utilities, described next.

3.2.3 Proportional Fair Utility

A tradeoff between the maximization of the sum rate and the maximization of the minimum rate could be the maximization of the geometric mean data rate. The geometric mean data rate for K users is given by:

$$R^{(\text{gm})} = \left(\prod_{k=1}^K R_k \right)^{1/K} \quad (13)$$

The metric (13) is fair, since a user with a data rate close to zero will make the whole product in $R^{(\text{gm})}$ go to zero. Hence, any RRM algorithm maximizing $R^{(\text{gm})}$ would avoid having any user with very low data rate. In addition, the metric (13) will reasonably favor users with good wireless channels (capable of achieving high data rate), since a high data rate will contribute in increasing the product in (13).

To be able to write the geometric mean in a sum-utility form as in (9), it can be noted that maximizing the geometric mean in (13) is equivalent to maximizing the product, which is equivalent to maximizing the sum of logarithms:

$$\begin{aligned} \max \prod_{k=1}^K R_k &\iff \max \ln \left(\prod_{k=1}^K R_k \right) \\ &= \max \sum_{k=1}^K \ln(R_k) \end{aligned} \quad (14)$$

Consequently, the algorithmic implementation of (14) can be handled by the algorithm of Section 4, by using, in that algorithm, $U_k = \ln(R_k)$ as the utility of user k , where \ln represents the natural logarithm. Maximizing the sum of logarithms in (14) is equivalent to maximizing the product and is easier to implement numerically. Hence, letting $U = \ln(R)$ provides proportional fairness [18, 19].

3.2.4 QoS-based Utility

The Max C/I, proportional fair (PF), and Max-Min utilities reflect the network performance, but do not indicate if a specific user has achieved a desired QoS level or not. For green network operation, maximizing either the sum-rate or the minimum rate, prevents by itself switching off certain FAPs. Instead, the objective in this case would be to maximize the number of users achieving their QoS requirements. Resources allocated to increase the data rates beyond these requirements would be redundant. Therefore, in this section, we propose a utility that reflects the number of users achieving a target data rate R_{th} , or how close they are to achieve it.

The utility function used for this purpose is expressed as follows:

$$U_{k_l} = 1_{R_{k_l} \geq R_{th}} + 1_{R_{k_l} < R_{th}} \frac{R_{k_l}}{R_{th}} \quad (15)$$

In (15), the notation $1_{(\text{Condition})}$ is used such that $1_{(\text{Condition})} = 1$ if condition is verified, and $1_{(\text{Condition})} = 0$ if the condition is not verified. This utility aims to maximize the number of users who exceed their target data rate threshold R_{th} (first term in (15)), or, if this is not achievable, reach a data rate as close as possible to R_{th} (second term in (15), which corresponds to the fraction of R_{th} achieved by the FUE). This utility is used with the Algorithm of Section 5 in order to obtain the results of Section 6.2.

4 Centralized RRM Algorithm

To perform the maximization of (9), we use the utility maximization algorithm, Algorithm 1, described in this section. This algorithm was first presented by the author in [1]. In this paper, the energy efficiency aspects are added and investigated through Algorithm 2 presented in Section 5, and the two algorithms are compared in the results section. Algorithm 1 can be applied with a wide range of utility functions, thus being able to achieve various objectives, with each objective represented by a certain utility function. Hence, it can be used for max C/I, PF, and Max-Min RRM, with the utilities derived in Section 3.2.

Lines 1-8 in Algorithm 1 are used for initialization. The loop in lines 10-21 determines the network utility enhancement that can be achieved by each (user, RB) allocation. The allocation leading to maximum enhancement (Line 22) is performed if it leads to an increase in network utility (Lines 23-30). After each allocation, the interference levels in the network vary. Hence, interference and data rates are updated and the novel utilities are computed. The process is repeated until no additional improvement can be obtained (Lines 9-34), with $I_{\text{Improvement}}$ being an indicator variable tracking if an improvement in network utility has been achieved ($I_{\text{Improvement}} = 1$) or not ($I_{\text{Improvement}} = 0$).

Algorithm 1 is implemented by the central controller in the scenario described in Section 2. In this paper, one user is considered to be active per femtocell. In the case where each FAP performs RRM in a distributed way (without wired connections to a central controller), then the maximization of the three utility types in each femtocell is achieved by allocating all the RBs of a given FAP to the active user. In fact, in this case, there would be no information about the channel gains and interference levels in the other femtocells. Thus, it makes sense for each FAP to try to maximize the QoS of its served user by allocating all available resources to that user. For a given FAP l , this corresponds, simultaneously, to maximizing the sum rate, maximizing the logarithm of the rate, and maximizing the minimum rate (In fact, with one user k_l present, R_{k_l} is the only rate and thus would correspond to the sum rate, the minimum rate, and the geometric mean data rate in cell l). This uncoordinated allocation will lead to an increase in interference levels, and to an overall degradation of performance in the network, as shown by the results of Section 6.

Algorithm 1 Utility Maximization Algorithm

```

1: for all FAP  $l$  and user  $k_l$  do
2:   for all RB  $j$  do
3:      $\alpha_{k_l,j}^{\text{old}} = 0$ 
4:      $U_{k_l}^{\text{old}}(\alpha^{\text{old}}) = 0$ 
5:   end for
6: end for
7:  $U_{\text{tot}}^{\text{old}} = \sum_{l=1}^L \sum_{k_l=1}^{K_l} U_{k_l}^{\text{old}}(\alpha^{\text{old}})$ 
8:  $I_{\text{Improvement}} = 1$ 
9: while  $I_{\text{Improvement}} = 1$  do
10:  for all FAP  $l$  and user  $k_l$  do
11:    for all RB  $j$  do
12:       $\alpha_{k_l,j}^{\text{new}} = \alpha_{k_l,j}^{\text{old}}$ 
13:       $\alpha_{k_l,j}^{\text{new}} = 1$ 
14:      for all FAP  $m$  and user  $k_m$  do
15:        Calculate the interference and achievable data rates in the network
16:        Calculate  $U_{k_m}^{\text{new}}(\alpha^{\text{new}})$ 
17:      end for
18:       $U_{\text{tot}}^{\text{new}} = \sum_{l=1}^L \sum_{k_l=1}^{K_l} U_{k_l}^{\text{new}}(\alpha^{\text{new}})$ 
19:       $\delta_{k_l,j} = U_{\text{tot}}^{\text{new}} - U_{\text{tot}}^{\text{old}}$ 
20:    end for
21:    end for
22:    Find  $(k^*, l^*, j^*) = \arg \max_{k,l,j} \delta_{k_l,j}$ 
23:    if  $\delta_{k^*,l^*,j^*} > 0$  then
24:       $\alpha_{k^*,l^*,j^*}^{\text{old}} = 1$ 
25:      for all FAP  $m$  and user  $k_m$  do
26:        Calculate the interference and achievable data rates in the network
27:        Calculate  $U_{k_m}^{\text{old}}(\alpha^{\text{old}})$ 
28:      end for
29:       $U_{\text{tot}}^{\text{old}} = \sum_{l=1}^L \sum_{k_l=1}^{K_l} U_{k_l}^{\text{old}}(\alpha^{\text{old}})$ 
30:       $I_{\text{Improvement}} = 1$ 
31:    else
32:       $I_{\text{Improvement}} = 0$ 
33:    end if
34: end while

```

It should be noted that Algorithm 1 allocates the resources of a given FAP exclusively to the FUE served by that FAP, i.e., it supports closed access operation, although it optimizes the performance by providing centralized control over the RRM process. In a green networking scenario, certain FAPs can be switched-off and their users served by other FAPs in order to save energy. Hence, an algorithm with open-access operation, allowing FAP switch off while meeting the QoS requirements of FUEs is required. Such an algorithm is presented in Section 5.

Algorithm 2 Green FAP Switch-Off Algorithm

```

1: for  $N_{\text{Rounds}} = 1$  to  $\text{MaxRounds}$  do
2:   for  $l = 1$  to  $L$  do
3:      $\delta_l = 0$ 
4:   end for
5:   Find  $l = \arg \min_{j; \xi_j=1, \delta_j=0} \sum_{k_j=1}^{K_j} \sum_{i=1}^{N_{\text{RB}}} \alpha_{k_j, i, j}$ 
6:    $k_l = 0$ 
7:    $\delta_l = 1$ 
8:    $\text{HO\_OK} = 1$ 
9:   while  $k_l < K_l$  AND  $\text{HO\_OK} = 1$  do
10:     $k_l = k_l + 1$ 
11:    Find  $j^* = \arg \max_{j; \xi_j=1} \sum_{i=1}^{N_{\text{RB}}} \gamma_{k_l, i, j}$ 
12:     $N_{\text{Attempts}} = 0$ 
13:     $R_{k_l} = 0$ 
14:    while  $(R_{k_l} < R_{\text{th}})$  AND  $(\sum_{i=1}^{N_{\text{RB}}} \alpha_{k_l, i, j^*} < N_{\text{RB}})$  AND  $(N_{\text{Attempts}} < \text{MaxAttempts})$ 
15:      do
16:         $N_{\text{Attempts}} = N_{\text{Attempts}} + 1$ 
17:        Find  $i^* = \arg \max_{i; \alpha_{k_l, i, j^*}=0} \gamma_{k_l, i, j^*}$ 
18:        Allocate RB  $i^*$  to FUE  $k_l$ :  $\alpha_{k_l, i^*, j^*} = 1$ 
19:        Calculate the rate of FUE  $k_l$  over RB  $i^*$ :  $R_{k_l, i^*}$ 
20:        Set  $R_{k_l} = R_{k_l} + R_{k_l, i^*}$ 
21:      end while
22:      if  $R_{k_l} \geq R_{\text{th}}$  then
23:        for all RB  $i$  such that  $\alpha_{k_l, i, l} = 1$  do
24:           $\alpha_{k_l, i, l} = 0$ 
25:        end for
26:         $\text{HO\_OK} = 1$ 
27:      else
28:        for all RB  $i$  such that  $\alpha_{k_l, i, j^*} = 1$  do
29:           $\alpha_{k_l, i, j^*} = 0$ 
30:        end for
31:         $\text{HO\_OK} = 0$ 
32:      end if
33:    end while
34:    if  $\text{HO\_OK} = 1$  AND  $\sum_{k_l=1}^{K_l} \sum_{i=1}^{N_{\text{RB}}} \alpha_{k_l, i, l} = 0$  then
35:       $\xi_l = 0$ 
36:    end if
37:  end for

```

4.1 Complexity Analysis

This section analyzes the complexity of Algorithm 1. The loop at line 10 has a complexity in the order of $L \cdot K_l$, whereas the loop at line 11 has a complexity in the order of N_{RB} . In addition, the loops at lines 14-17 and 25-28 have a complexity in the order of $L \cdot K_l$. Thus, the complexity is in the order of: $L \cdot K_l [N_{\text{RB}} \cdot (L \cdot K_l)] + L \cdot K_l$. Denoting by N_{imp} the number of iterations with improvements in the main loop of the algorithm (starting at line 9), the complexity becomes: $[L \cdot K_l [N_{\text{RB}} \cdot (L \cdot K_l)] + L \cdot K_l] \cdot N_{\text{imp}}$. With N_{imp} generally being in the order of $L \cdot K_l$, it becomes straightforward to show that the complexity of Algorithm 1 is in the order of $\mathcal{O}(L^3 \cdot K_l^3 \cdot N_{\text{RB}})$, which is polynomial in the number of FAPs, users per FAP, and RBs.

5 Green FAP Switching Algorithm

To perform centralized energy efficient operation of the femtocell network, the proposed Algorithm 2, described in this section, is used. Algorithm 2 is implemented by the central controller in the scenario described in Section 2. In this paper, one FUE is considered to be active per femtocell, although Algorithm 2 is applicable with any number of FUEs per femtocell. An FUE is considered to be successfully served if it achieves a data rate above a defined threshold R_{th} .

In the algorithm, δ_l is a tracking parameter used to track if an attempt has been made to switch off FAP l . It is set to $\delta_l = 1$ if an attempt was made and to $\delta_l = 0$ otherwise. ξ_l is a parameter indicating if FAP l is switched on or off. It is set to $\xi_l = 1$ if the FAP is active and to $\xi_l = 0$ if it is switched off. In this paper, we set $\text{MaxRounds} = L$ and $\text{MaxAttempts} = N_{RB}$.

The algorithm finds the FAP that has the lowest load, with the load defined in this paper as the number of allocated RBs in the FAP (Line 5). It then makes an attempt to switch off this FAP by moving its served FUEs to neighboring active FAPs (Loop at Lines 9-32). The algorithm finds for each FUE, the best serving FAP other than the current FAP l , in terms of best average SINR (Line 11). If the FUE can be successfully handed over to the target FAP (and it can achieve its target rate after resource allocation at Lines 14-20), it is handed over and the handover parameter HO_OK is set to 1 (Lines 21-25). If at least one FUE cannot be handed over, HO_OK is set to 0 and FAP l remains on after freeing any reserved RBs in the target FAP (Lines 27-30). When all FUEs are handed over successfully, FAP l can be switched off (Lines 33-35). Otherwise, if at least one FUE was not served successfully, FAP l remains active.

5.1 Complexity Analysis

This section analyzes the complexity of Algorithm 2. In order to switch FAP l off, the algorithm attempts to find another FAP to serve k_l , for each FUE k_l served by FAP l . This process has a complexity in the order of $K_l \cdot (L - 1)$, since the search can involve at most $(L - 1)$ FAPs, when all FAPs other than FAP l are still switched on. This number will decrease as more FAPs are switched off. RB allocation has to be performed in the new FAP for FUE k_l . The loop at lines 14-20 handles this process, and thus the complexity becomes $N_{RB} \cdot K_l \cdot (L - 1)$. The number of attempts made in this process cannot exceed the number of RBs. Hence, the complexity becomes: $N_{RB} \cdot K_l \cdot (L - 1) \cdot \min(N_{RB}, \text{MaxAttempts})$. This whole process is repeated for MaxRounds , and hence the complexity of Algorithm 2 is: $N_{RB} \cdot K_l \cdot (L - 1) \cdot \min(N_{RB}, \text{MaxAttempts}) \cdot \text{MaxRounds}$. Considering the worst case scenario $\text{MaxAttempts} = N_{RB}$, and making one switch-off attempt on each of the FAPs (i.e., setting $\text{MaxRounds} = L$), it becomes straightforward to show that the complexity of Algorithm 2 is in the order of $\mathcal{O}(L^2 \cdot N_{RB}^2 \cdot K_l)$, which is polynomial in the number of FAPs, users per FAP, and RBs.

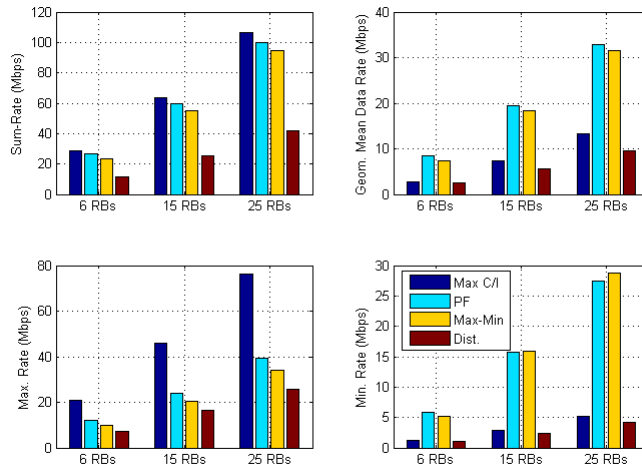


Fig. 3 Results in the case of one floor (three femtocells).

In terms of signaling complexity, it should be noted that such an algorithm will require significant feedback overhead in a distributed scenario, where the FAPs would have to exchange large amounts of signaling information in order to coordinate their transmissions without a central controller. However, in the system model considered in this paper and shown in Fig. 1, a centralized scenario is investigated. Hence, FAPs only have to receive standard LTE signaling from FUEs over the air interface, and relay this signaling information over the wired network to the central controller. This controller will run Algorithm 2, and will consequently inform the FAPs to allocate RBs to FUEs and whether to go into sleep mode or not. Thus, the whole FAP network with centralized control would be operating as a single BS (central controller) having a distributed antenna system (DAS), with the FAPs behaving like remote antenna heads (RAHs), albeit with increased intelligence compared to traditional RAHs.

6 Results and Discussion

This section presents the Matlab^(c) simulation results obtained by implementing the proposed approach under the system model of Section 2. We consider a building as shown in Fig. 1. Three apartments per floor are assumed, with one active user per apartment using the FAP to access the network (assuming one FAP per apartment). The maximum FAP transmit power is set to 1 Watt, whereas the transmit power of the macro BS is set to 10 Watts.

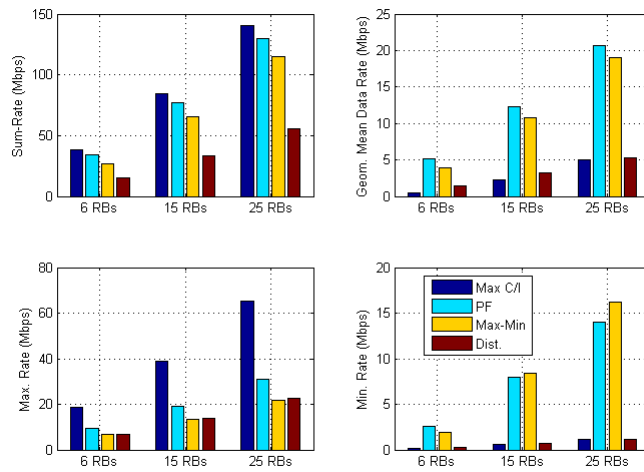


Fig. 4 Results in the case of two floors (six femtocells).

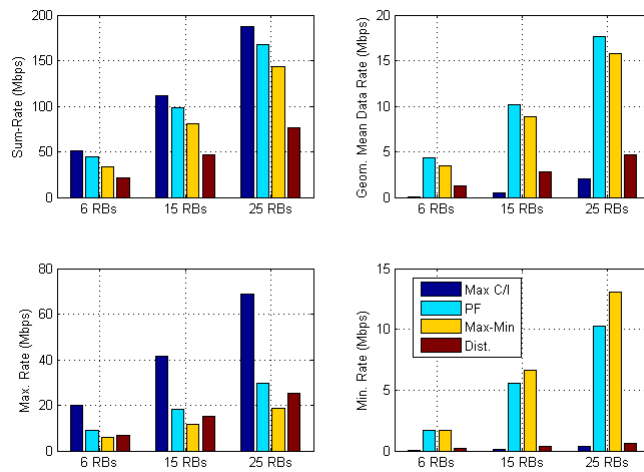


Fig. 5 Results in the case of three floors (nine femtocells).

6.1 Results of Centralized RRM with all the FAPs Active

This section presents the results of implementing Algorithm 1 described in Section 4 when all the FAPs are active. Scenarios with one floor only (three apartments on ground floor), two floors (six apartments), and three floors (nine apartments) are investigated, with the results shown in Figs. 3, 4, and 5, respectively.

The figures show that max C/I scheduling leads to the highest sum-rate in the network. However, this comes at the expense of fairness, as it can be seen from the geometric mean results of max C/I . In fact, the bottom subfigures of Figs. 3 to 5 show that max C/I enhances the maximum rate in the network, by allocating most of the resources to the user having the best channel and interference conditions, while depriving other users from sufficient resources, thus leading to unfairness, as shown by the minimum rate plots. On the other hand, PF scheduling maximizes the geometric mean for all the investigated scenarios. Clearly, the minimum rates achieved with PF indicate that a PF utility is significantly more fair than max C/I . The results of Max-Min scheduling also show a fair performance. In fact, Max-Min resource allocation leads to maximizing the minimum rate in the network for almost all the studied scenarios, except in the case of one and two floors with six RBs, where it is slightly outperformed by PF. This is due to the approximation performed by taking, in (12), $a = 10$ instead of $a = \infty$. When the number of resources increases to 15 and 25 RBs, the algorithm has additional flexibility to implement RRM with Max-Min such that the minimum rate is maximized compared to the other methods. It can also be noted that Max-Min scheduling leads to a geometric mean performance that is reasonably close to that of PF scheduling, indicating that it also enhances overall fairness in the network. Figs. 3 to 5 also show that, as expected, the data rates increase for all the studied metrics when the number of RBs increases.

Comparing the joint wired/wireless case to the distributed scenario where each FAP performs RRM independently without centralized control, it can be seen that the distributed scenario is outperformed by the integrated wired/wireless approach for all the investigated metrics: Max C/I leads to a higher sum-rate, PF leads to a higher geometric mean, and Max-Min leads to a higher minimum rate. This is due to the fact that with distributed RRM, a FAP is not aware of the interference conditions to/from other FAPs and users. This leads to a severe performance degradation, as can be seen in Figs. 3 to 5, although all the RBs of a given FAP are allocated to the user served by that FAP.

6.2 Results of the Green Network Operation with FAP On/Off Switching

This section presents the simulation results, considering the scenario of Fig. 1, with different values for R_{th} and the available LTE bandwidth. The following methods are compared:

- The centralized scheduling algorithm presented in Section 4. It assumes each FAP serves only its corresponding FUEs without taking energy efficiency into account. But the resource allocation is performed by the central controller, which allows to avoid interference.
- The “selfish” approach, where each FBS allocates all its RBs to the FUE it is serving, regardless of the allocations in other cells. This scenario assumes neither centralized control, nor any form of coordination between FAPs. Thus, it would be logical for each FAP to allocate all resources to its served FUEs, given that no other coordination or interference information is available.

Table 1 Average Data Rates (Mbps)

	Centralized	Green Centralized	Selfish
$N_{\text{RB}} = 15$ $R_{\text{th}} = 2$ Mbps	2.74	3.01	5.25
$N_{\text{RB}} = 15$ $R_{\text{th}} = 5$ Mbps	6.01	6.06	5.25
$N_{\text{RB}} = 15$ $R_{\text{th}} = 7$ Mbps	7.64	7.18	5.25
$N_{\text{RB}} = 15$ $R_{\text{th}} = 10$ Mbps	9.44	8.94	5.25
$N_{\text{RB}} = 25$ $R_{\text{th}} = 5$ Mbps	6.09	6.14	8.54
$N_{\text{RB}} = 25$ $R_{\text{th}} = 7$ Mbps	7.82	7.87	8.54
$N_{\text{RB}} = 25$ $R_{\text{th}} = 10$ Mbps	10.94	10.91	8.54
$N_{\text{RB}} = 50$ $R_{\text{th}} = 10$ Mbps	11.00	11.04	15.90

Table 2 Geometric Mean Data Rates (Mbps)

	Centralized	Green Centralized	Selfish
$N_{\text{RB}} = 15$ $R_{\text{th}} = 2$ Mbps	2.15	2.94	2.83
$N_{\text{RB}} = 15$ $R_{\text{th}} = 5$ Mbps	5.83	6.00	2.83
$N_{\text{RB}} = 15$ $R_{\text{th}} = 7$ Mbps	7.46	6.57	2.83
$N_{\text{RB}} = 15$ $R_{\text{th}} = 10$ Mbps	8.84	6.01	2.83
$N_{\text{RB}} = 25$ $R_{\text{th}} = 5$ Mbps	5.92	6.07	4.66
$N_{\text{RB}} = 25$ $R_{\text{th}} = 7$ Mbps	7.70	7.83	4.66
$N_{\text{RB}} = 25$ $R_{\text{th}} = 10$ Mbps	10.84	10.78	4.66
$N_{\text{RB}} = 50$ $R_{\text{th}} = 10$ Mbps	10.91	11.01	8.56

- The approach proposed in Algorithm 2, where, starting from an initial allocation without energy efficiency obtained by implementing Algorithm 1, the proposed Algorithm 2 implements centralized FAP switching off after offloading FUEs to active FAPs that can maintain their QoS.

In this section, we use a capped capacity formula in order to limit the possibility of users to achieve their target rate:

$$R_{k_l}(\mathbf{P}_1, \mathcal{I}_{\text{sub}, k_l}) = \max \left(\sum_{i \in \mathcal{I}_{\text{sub}, k_l}} B_{\text{sub}} \cdot \log_2(1 + \beta \gamma_{k_l, i, l}), R_{\text{max}} \right) \quad (16)$$

Table 3 Fraction of Users in Outage

	Centralized	Green Centralized	Selfish
$N_{\text{RB}} = 15$ $R_{\text{th}} = 2$ Mbps	0.16	0.0	0.36
$N_{\text{RB}} = 15$ $R_{\text{th}} = 5$ Mbps	0.11	0.0	0.62
$N_{\text{RB}} = 15$ $R_{\text{th}} = 7$ Mbps	0.15	0.13	0.73
$N_{\text{RB}} = 15$ $R_{\text{th}} = 10$ Mbps	0.55	0.44	0.83
$N_{\text{RB}} = 25$ $R_{\text{th}} = 5$ Mbps	0.11	0	0.46
$N_{\text{RB}} = 25$ $R_{\text{th}} = 7$ Mbps	0.11	0	0.57
$N_{\text{RB}} = 25$ $R_{\text{th}} = 10$ Mbps	0.10	0.01	0.68
$N_{\text{RB}} = 50$ $R_{\text{th}} = 10$ Mbps	0.11	0	0.49

Table 4 Fraction of Active FAPs

	Centralized	Green Centralized	Selfish
$N_{\text{RB}} = 15$ $R_{\text{th}} = 2$ Mbps	1	0.11	1
$N_{\text{RB}} = 15$ $R_{\text{th}} = 5$ Mbps	1	0.11	1
$N_{\text{RB}} = 15$ $R_{\text{th}} = 7$ Mbps	1	0.12	1
$N_{\text{RB}} = 15$ $R_{\text{th}} = 10$ Mbps	1	0.21	1
$N_{\text{RB}} = 25$ $R_{\text{th}} = 5$ Mbps	1	0.11	1
$N_{\text{RB}} = 25$ $R_{\text{th}} = 7$ Mbps	1	0.11	1
$N_{\text{RB}} = 25$ $R_{\text{th}} = 10$ Mbps	1	0.11	1
$N_{\text{RB}} = 50$ $R_{\text{th}} = 10$ Mbps	1	0.11	1

Compared to (5), the expression in (16) is a capped Shannon formula; i.e., the data rate is not allowed to exceed the maximum limit R_{max} that can be reached using practical modulation and coding schemes (MCS) in LTE. This limit is determined as follows:

$$R_{\text{max}} = \frac{r_n \cdot N_{\text{RB}}^{(k_l)} \cdot N_{\text{SC}}^{\text{RB}} \cdot N_{\text{Symb}}^{\text{SC}} \cdot N_{\text{Slot}}^{\text{TTI}}}{T_{\text{TTI}}}, \quad (17)$$

where r_n is the rate in bits/symbol corresponding to the MCS used over the subcarriers of the RBs allocated to the user. R_{max} is obtained with $r_n = 6$ corresponding to uncoded 64-QAM, the highest MCS used in LTE. In addition, $N_{\text{RB}}^{(k_l)}$ is the number of

Table 5 Normalized Utility

	Centralized	Green Centralized	Selfish
$N_{RB} = 15$ $R_{th} = 2$ Mbps	0.90	1.0	0.79
$N_{RB} = 15$ $R_{th} = 5$ Mbps	0.97	1.0	0.62
$N_{RB} = 15$ $R_{th} = 7$ Mbps	0.97	0.92	0.53
$N_{RB} = 15$ $R_{th} = 10$ Mbps	0.90	0.76	0.44
$N_{RB} = 25$ $R_{th} = 5$ Mbps	0.98	1	0.72
$N_{RB} = 25$ $R_{th} = 7$ Mbps	0.98	1	0.65
$N_{RB} = 25$ $R_{th} = 10$ Mbps	0.98	0.99	0.56
$N_{RB} = 50$ $R_{th} = 10$ Mbps	0.99	1	0.70

RBs allocated to k_l , N_{SC}^{RB} is the number of subcarriers per RB (equal to 12 in LTE), N_{Symb}^{SC} is the number of symbols per subcarrier during one time slot (set to six or seven in LTE, depending whether an extended cyclic prefix is used or not), N_{Slot}^{TTI} is the number of time slots per TTI (two 0.5ms time slots per TTI in LTE), and T_{TTI} is the duration of one TTI (1ms in LTE) [13].

We use the utility (15) with both Algorithms 1 and 2. The average data rate results are shown in Table 1. However, the average rate results alone can be misleading. In fact, when an FUE A has a very high data rate while another FUE B has a very poor data rate, the average might still be high, but the poor performance of FUE B is masked by the high rate of FUE A. Using the geometric mean results provides a better indication of fairness. The geometric mean data rate results are presented in Table 2. In addition, Table 3 shows the fraction of FUEs in outage, i.e. the number of FUEs that did not achieve R_{th} divided by the total number of FUEs. Table 4 shows the fraction of FAPs that are active in order to serve the FUEs. Naturally, the centralized and selfish cases have all their values equal to 1, since 100% of the FAPs are active. Table 5 shows the value of the utility function (15).

Tables 1-5 show that the centralized scheduling approach and the centralized green approach significantly outperform the selfish method, especially in terms of fairness and outage. The results of Table 4 indicate that the proposed green method of Algorithm 2 is achieving significant energy savings, as it is using only one or two FAPs to serve the nine FUEs (indeed, the value 0.11 corresponds to the ratio 1/9). This is an interesting result, since it indicates that FUEs in neighboring apartments can be successfully served by a single FAP, which saves around 90 % of FAP energy consumption.

Comparing the results of Algorithm 1 to Algorithm 2, Tables 1, 2, and 5 show that they have a comparable performance, with one being slightly better than the other, or vice versa. However, interestingly, Table 3 shows that Algorithm 2 always leads to better outage performance. This is explained by the fact, that, although fully central-

ized and using all FAPs, Algorithm 1 operates under the constraint that a FAP serves only the FUEs in its apartment. Hence, although centralized control allows mitigating interference and a joint selection of suitable RBs in all FAPs, this approach disregards certain scenarios where fading is constructive with other FAPs, leading occasionally to better channels when an FUE is served by the FAP of another apartment. With the proposed green method, this constraint is relaxed since the purpose is to offload FUEs in order to switch FAPs off. Furthermore, switching off certain FAPs for energy efficiency has the desirable side effect of reducing the interference in the network, due to shutting down some (or in the simulated scenario, most) of the transmitters. Indeed, Algorithm 2 starts from an initial implementation of Algorithm 1, followed by an enhancement operation consisting of FAP switch off in order to reduce the energy consumption in the network.

7 Conclusions

In this paper, radio resource management and green operation in LTE femtocell networks with centralized control was investigated. The studied scenario consisted of an integrated wired/wireless system, where the femtocell access points are controlled by a single entity. This permits performing joint radio resource management in a centralized and controlled way in order to enhance the quality of service performance for all users in the networks. It also allows an energy efficient operation of the network by switching off redundant femtocells whenever possible. Two algorithms were proposed and analyzed. The first one is a utility maximizing radio resource management algorithm. It was used to maximize different utility functions leading to different target objectives in terms of network sum-rate, fairness, and enhancing the worst-case performance in the network. The second algorithm is FAP switch off algorithm, implemented at the central controller. The joint wired/wireless resource management approach was compared to the distributed resource management case, where each femtocell acts as an independent wireless network unaware of the channel and interference conditions with the other cells. The integrated wired/wireless approach led to significant gains compared to the wireless only case, and the performance trade-offs between the various utility functions were analyzed and assessed. The results of the green algorithm showed significant energy savings while satisfying QoS requirements.

Acknowledgements The author would like to thank the Editor and the Reviewers for their feedback and comments, which helped in increasing the clarity and quality of this paper.

References

1. E. Yaacoub, "Radio Resource Management in Integrated Wired/Wireless LTE Femtocell Networks", in *Proc. of the 12th International Conference on Wired and Wireless Internet Communications*, Paris, France, May 2014.
2. J. G. Andrews, H. Claussen, M. Dohler, S. Rangan, and M. C. Reed, "Femtocells: Past, Present, and Future", *IEEE Journal on Selected Areas in Communications*, vol. 30, no. 3, pp. 497–508, 2012.

3. V. Chandrasekhar, J. G. Andrews, and A. Gatherer, "Femtocell Networks: A Survey", *IEEE Communications Magazine*, vol. 46, no. 9, pp. 59–67, 2008.
4. D. Knisely, T. Yoshizawa, and F. Favichia, "Standardization of Femtocells in 3GPP", *IEEE Communications Magazine*, vol. 47, no. 9, pp. 68–75, 2009.
5. V. Chandrasekhar, M. Kountouris, and J. G. Andrews, "Coverage in Multi-Antenna Two-Tier Networks", *IEEE Transactions on Wireless Communications*, vol. 8, no. 10, pp. 5314–5327, 2009.
6. F. Pantisano, M. Bennis, W. Saad, and M. Debbah, "Spectrum Leasing as an Incentive towards Uplink Macrocell and Femtocell Cooperation", *IEEE Journal on Selected Areas in Communications*, vol. 30, no. 3, pp. 617–630, 2012.
7. C. Gussen, V. Belmega, and M. Debbah, "Pricing and Bandwidth Allocation Problems in Wireless Multi-Tier Networks", in *Proc. of Asilomar Conference on Signals Systems and Computers*, pp. 1633–1637, 2011.
8. S.-Y. Lien, C.-C. Tseng, K.-C. Chen, and C.-W. Su, "Cognitive Radio Resource Management for QoS Guarantees in Autonomous Femtocell Networks", in *Proc. of the IEEE International Conference on Communications, (ICC 2010)*, pp. 1–6, 2010.
9. S. Hong, C.-Y. Oh, and T.-J. Lee, "Resource Allocation Method Using Channel Sensing and Resource Reuse for Cognitive Femtocells", *International Journal of Information and Electronics Engineering*, vol. 3, no. 3, pp. 309–312, 2013.
10. M. A. Abdelmonem, M. Nafie, M. H. Ismail, and M. S., El-Soudani, "Optimized Spectrum Sensing Algorithms for Cognitive LTE Femtocells", *EURASIP Journal on Wireless Communications and Networking*, vol. 2012, no. 6, 19 pages (Open Access), 2012.
11. S. F. Hasan, N. H. Siddique, S. Chakraborty, "Femtocell versus WiFi - A survey and comparison of architecture and performance", in *Proc. of Wireless VITAE*, pp. 916–920, May 2009.
12. A. Mukherjee, J.-F. Cheng, S. Falahati, H. Koorapaty, D. H. Kang, R. Karaki, L. Falconetti, and D. Larsson, "Licensed-Assisted Access LTE: Coexistence with IEEE 802.11 and the Evolution toward 5G", *IEEE Communications Magazine*, vol. 54, no. 6, pp. 50–57, June 2016.
13. 3rd Generation Partnership Project (3GPP), 3GPP TS 36.211 3GPP TSG RAN Evolved Universal Terrestrial Radio Access (E-UTRA) Physical Channels and Modulation, version 13.1.0, Release 13, March 2016.
14. 3rd Generation Partnership Project (3GPP), 3GPP TS 36.213 3GPP TSG RAN Evolved Universal Terrestrial Radio Access (E-UTRA) Physical layer procedures, version 13.1.1, Release 13, March 2016.
15. Qualcomm Inc., 3GPP TSG-RAN WG1 #72 R1-130598, Agenda item: 7.3.7, "Channel Models for D2D Deployments", St. Julian's, Malta, 2013.
16. X. Qiu, and K. Chawla, "On the Performance of Adaptive Modulation in Cellular Systems", *IEEE Transactions on Communications*, vol. 47, no. 6, pp. 884–895, 1999.
17. J.-Y. Le Boudec, "Rate adaptation, Congestion Control and Fairness: A Tutorial", Tech. Report, Ecole Polytechnique Federale de Lausanne (EPFL), Lausanne, Switzerland, 2008.
18. G. Song, and Y. Li, "Cross-Layer Optimization for OFDM Wireless Networks-Part I: Theoretical Framework", *IEEE Transactions on Wireless Communications*, vol. 4, no. 2, pp. 614–624, 2005.
19. E. Yaacoub and Z. Dawy, "Resource Allocation in Uplink OFDMA Wireless Systems: Optimal Solutions and Practical Implementations", John Wiley and Sons / IEEE press, NY, ISBN: 978-1-1180-7450-3, 2012.